Rhesus macaques can be effectively infected with SARS-CoV-2 via ocular conjunctival route

Wei Deng[†,1], Linlin Bao[†,1], Hong Gao[†,1], Zhiguang Xiang[†,1], Yajin Qu[†,1], Zhiqi Song[†,1], Shunran Gong[†,1], Jiayi Liu[2], Jiangning Liu[1], Pin Yu[1], Feifei Qi[1], Yanfeng Xu[1], Fengli Li[1], Chong Xiao[1], Qi Lv[1], Jing Xue[1], Qiang Wei[1], Mingya Liu[1], Guanpeng Wang[1], Shunyi Wang[1], Haisheng Yu[1], Xing Liu[1], Wenjie Zhao[1], Yunlin Han[1], Chuan Qin[*,1]

[1] Key Laboratory of Human Disease Comparative Medicine, Chinese Ministry of Health, Beijing Key Laboratory for Animal Models of Emerging and Remerging Infectious Diseases, Institute of Laboratory Animal Science, Chinese Academy of Medical Sciences and Comparative Medicine Center, Peking Union Medical College, Beijing, China.

[2] Department of Radiology, Bejing Anzhen Hospital, Capital Medical University, Beijing, China.

†These authors contributed equally to this work.

*Correspondence should be addressed to Chuan Qin, Email: qinchuan@pumc.edu.cn.

Abstract: The outbreak of Corona Virus Disease 2019 (COVID-19) is highly infectious and transmitted mainly through human-to-human transmission via respiratory droplets and direct or close contact to the patients with SARS-CoV-2. The other potential transmission routes remain to be further researched. In some clinical cases, samples of tears and conjunctival secretions from both SARS-CoV[1] and SARS-CoV-2 patients with conjunctivitis[2] displayed detectable viral RNA. A previous study reported the case of a clinician who was infected with SARS-CoV-2 while working with patients under all safeguards except eye protection [2]. By contrast, no SARS-CoV-2 could be detected by RT-PCR in 114 conjunctival swabs samples from patients with COVID-19 pneumonia [4]. Anatomically, the linkage of the ocular with respiratory tissues is primarily by the nasolacrimal system [5]. The potential extra-respiratory transmissible routes of SARS-CoV-2 via ocular remained unclear. Whether ocular conjunctiva is one of the portals that SARS-CoV-2 enters the host needs to be further research by laboratory-confirmation for providing significant data to oversight and prevention in people.

Three rhesus macaques between the ages of 3 and 5 years were inoculated with 1×10^6 50% tissue-culture infectious doses ($TCID_{50}$) of SARS-CoV-2. Two of them were randomly selected to apply for ocular conjunctival inoculation, the remaining one macaque was inoculated via intratracheal route as a comparison to compare the distribution and pathogenesis of viruses in infected-host via different routes. Based on the clinical symptoms, viral load detection, and serological examination, we tested

whether rhesus macaque can be infected with SARS-CoV-2 via ocular conjunctival routes.

We daily observed the macaques for clinical signs. There was no significant clinical change in the body weight (Fig1A) and the temperature (Fig1B) of the inoculated macaques via both routes. Routine specimens, including nose swabs and throat swabs, were collected on 0, 1, 3, 5, and 7-day post-inoculation (dpi). Additionally, conjunctival swabs and anal swabs were also gathered to explore the potentially excretory routes of SARS-CoV-2 in the host. Remarkably, viral load can be tested in conjunctival swabs on 1 dpi via ocular conjunctival route and then became undetectable implying that the inoculated-SARS-CoV-2 may be transferred from conjunctiva to respiratory tract and other tissues. All three animals were able to detect a continued viral load in their nose swabs and throat swabs from 1 to 7 dpi. For anal swabs, although the viral load was undetectable in the conjunctival inoculated-animals, it can be ongoingly examined in the macaque inoculated via the intratracheal route (Fig1C).

The intratracheal inoculated-macaque and one of the conjunctival inoculated-animal were euthanized and necropsied on 7 dpi. For conjunctival route, viral load was primarily distributed in the nasolacrimal system and ocular, including the lacrimal gland, optic nerve, and conjunctiva nasal cavity; in the nose, including the nasal

mucosa, nasal turbinate, and nostril; in the pharynx including epiglottis, soft palate, and trachea; in the oral cavity including check pouch and parotid gland; as well as in other tissues including lower left lobe of the lung, inguinal and para (peri) rectal lymph node, stomach, duodenum, caecum, and ileum (Fig. 1D). By contrast, the distribution of viral might be somewhat different via intratracheal inoculation that viral replication was mainly in the lung, and viral load was also relative high in the nasal septum, tracheas, mandibular lymph node, tonsil, pulmonary lymph node, and some segments of the alimentary tract including caecum, colon, duodenum and jejunum (Fig. 1D). The diverse distributions of viruses by different inoculation routes were consistent with the anatomical structure. Notably, viruses were detectable in different segments of the alimentary canal revealing that the digestive system might be vulnerable and susceptible to SARS-CoV-2. Furthermore, the specific IgG antibody against SARS-CoV-2 was detectable in the conjunctival inoculated-macaque at 14 and 21 dpi proofing that the animal was infected with SARS-CoV-2 (Fig. 1E).

These data suggested that macaques can be infected with SARS-CoV-2 via the conjunctival route. By comparison, viral load and distribution in the conjunctival infected-macaque represented comparatively high in the nasolacrimal system but relatively mild and local in the lung compared with that in the macaque that inoculated via intratracheal routes. Similarly, both the two routes can cause alimentary canal infection.

We inoculated rhesus monkeys via a single route via conjunctiva to avoid multiple routes of co-inoculation for confirming the exact pathway of inoculation. These results suggest that conjunctiva is a portal for viral transmission. In our results, viral load can be detectable in several nasolacrimal system associated-tissues，especially in the conjunctiva, lacrimal gland, nasal cavity and throat, which outlined the anatomical bridge between ocular and respiratory tissues. Particularly, the lacrimal duct functions as a conduit to collect and transport tear fluid from the ocular surface to the nasal-inferior meatus, being convenient for the drainage of the virus from ocular to respiratory tract tissues. Actually, the previous report had demonstrated that although virus-containing fluid can be taken up through the conjunctiva, sclera, or cornea, the majority of liquid including tear and secretions is drained into the nasopharyngeal space or swallowed; the lacrimal duct epithelia are also possible to contribute to the absorption of tear fluid. Our results were highly consistent with the anatomical features that viruses enter the host via the conjunctival route. At present, people mainly wear masks to protect against SARS-CoV-2. This method mainly protects the nasal and oral mucosa. Conjunctiva exposed to the environment is easily overlooked. Respiratory viruses can stimulate ocular complications in infected patients, which then leads to respiratory infection [5]. The fact that exposed mucous membranes and unprotected eyes increased the risk of SARS-CoV[1] or SARS-CoV-2[2] transmission suggests that increase the awareness of eye protection is necessary, through regular hand-washing in daily life and wearing protective eyewear in close contact with the

patients or crowded places, especially for the clinicians. Only cutting off the transmission of SARS-CoV-2 we can effectively prevent the spread of COVID-19.

Materials and methods

Ethics statement

The animal biosafety level 3 (ABSL3) facility in the Institute of Laboratory Animal Science was used to complete all the experiments with rhesus macaques infection doing with HEPA-filtered isolators. The Institutional Animal Care and Use Committee of the Institute of Laboratory Animal Science, Peking Union Medical College, examined and authorized all the programs in this research including animals (BLL20001).

Cells and Viruses

The SARS-CoV-2 named SARS-CoV-2/WH-09/human/2020/CHN was isolated by the Institute of Laboratory Animal Science, Peking Union Medical College. Vero cells were applied to the reproduction of SARS-CoV-2 stocks. Dulbecco's modified Eagle's medium (DMEM, Invitrogen, Carlsbad, USA) were applied to incubate this cell line at 37°C, 5% CO_2, complemented with 10% fetal bovine serum (FBS), 100 μg/ml streptomycin, and 100 IU/ml penicillin, and maintained. Titers for SARS-CoV-2 were resolved by $TCID_{50}$ assay.

127 ***RNA extraction and RT-PCR***

128 All the collected-organs were applied to extract Total RNA as the description in the
129 previous report. Briefly, the RNeasy Mini Kit from Qiagen, Hilden, Germany and the
130 PrimerScript RT Reagent Kit from TaKaRa, Japan were used following manufacturer
131 instructions. RT-PCR reactions were applied to the PowerUp SYBG Green Master
132 Mix Kit from Applied Biosystems, USA, following cycling protocol: 50°C for 30 min,
133 followed by 40 cycles at 95℃ for 15 min, 94°C for 15 s, and 60°C for 45 s. The
134 primer sequences used for RT-PCR were targeted against the envelope (E) gene of
135 SARS-CoV-2. The forward primer is 5'-TCGTTTCGGAAGAGACAGGT-3', the
136 reverse primer is 5'-GCGCAGTAAGGATGGCTAGT-3'.

137

138 ***Animal experiments***

139 Two male rhesus macaques (3–5 years old) were inoculated with 10^6 $TCID_{50}$/ml
140 SARS-CoV-2 via ocular conjunctival routes and one was inoculated via intratracheal
141 routes in sequence, respectively. On 0, 1, 3, 5, and 7 dpi, the conjunctival, nasal,
142 throat and anal swabs were collected and incubated in 1 ml DMEM with 50 μg/ml
143 streptomycin and 50 U/ml penicillin. The IPTT-300 temperature probes, which were
144 injected interscapular into the macaques before the start of the experiment, were
145 applied to do temperature monitor every day. Tissues were collected as followed,
146 conjunctiva, lacrimal gland, optic nerve, cerebellum, cerebrum, different segments of
147 the spinal cord, nostril, nasal turbinate, nasal mucosa, soft palate, cheek pouch,
148 parotid gland, epiglottis, lingual tonsil, pharyngeal tonsil, different lobes of lung,
149 trachea, different lymph nodes, heart, liver, spleen, pancreas, alimentary canal, kidney,
150 bladder, and brown adipose tissues samples for detecting the viral loads. All sera were

151 collected on 0, 7, 14 and 21 dpi for serologic detection to exam whether there
152 presence the IgG antibodies reactive with SARS-CoV-2 antigens.

153

154 ***Preparation of Homogenate Supernatant***

155 An electric homogenizer was applied to prepare tissues homogenates by 2 min 30s
156 incubated in 1ml of DMEM. The homogenates were centrifuged at 3,000 rpm at 4°C
157 for 10 min. The supernatant was harvested and reposited for viral titer at −80°C.

158

159 ***ELISA antibody assay***

160 Sera of Each animal were collected to detect the SARS-CoV-2 antibody through
161 enzyme-linked immunosorbent assay (ELISA) on 0, 3, 7, 11, and 14 dpi. The 96-well
162 plates coated with 0.1μg Spike protein of SARS-CoV-2 from Sino Biological (Product
163 code: 40591-V08H) at 4□ overnight were blocked by 2% BSA/PBST at room
164 temperature for 1 hour. Sera samples were diluted at 1:100, and then were added to
165 different wells and maintained at 37℃for 30 minutes, followed by the goat
166 anti-mouse antibody labeled with horseradish peroxidase (Beijing ZSGB
167 Biotechnology, ZB-2305) incubated at room temperature for 30 minutes. The OD450
168 value of sera from each of the animals was at least twice more than the negative
169 control was regarded as reacting with SARS-CoV-2 antigen and positive result.

170

171 ***Statistical analysis***

Between the two groups, the statistically significant differences were confirmed by unpaired Student's *t*-tests. All data were analyzed with GraphPad Prism 8.0 software.

Acknowledgements

This work was supported by the CAMS Initiative for Innovative Medicine of China (Grant No. 2016-I2M-2-006) and National Mega projects of China for Major Infectious Diseases (Grant No. 2017ZX10304402).

Competing interests

The authors have no competing interests to declare.

References:

1. Chan WM, Yuen K, Fan D, Lam D, Chan P and Sung J. Tears and conjunctival scrapings for coronavirus in patients with SARS. Brit J Ophthalmol. 2004; 88(7):968-969

2. Xia J, Tong J, Liu M, Shen Y and Guo D. Evaluation of coronavirus in tears and conjunctival secretions of patients with SARS-CoV-2 infection. J Med Virol. 2020;

3. Lu C, Liu X and Jia Z. 2019-nCoV transmission through the ocular surface must not be ignored. The Lancet. 2020; 395(10224):e39

4. Deng C, Yang Y, Chen H, Chen W, Chen Z, Ma K and Wang J. Ocular Dectection of SARS-CoV-2 in 114 Cases of COVID-19 Pneumonia in Wuhan, China: An Observational Study. China: An Observational Study (2/19/2020). 2020;

5. Belser JA, Rota PA and Tumpey TM. Ocular tropism of respiratory viruses. Microbiol. Mol. Biol. Rev. 2013; 77(1):144-156

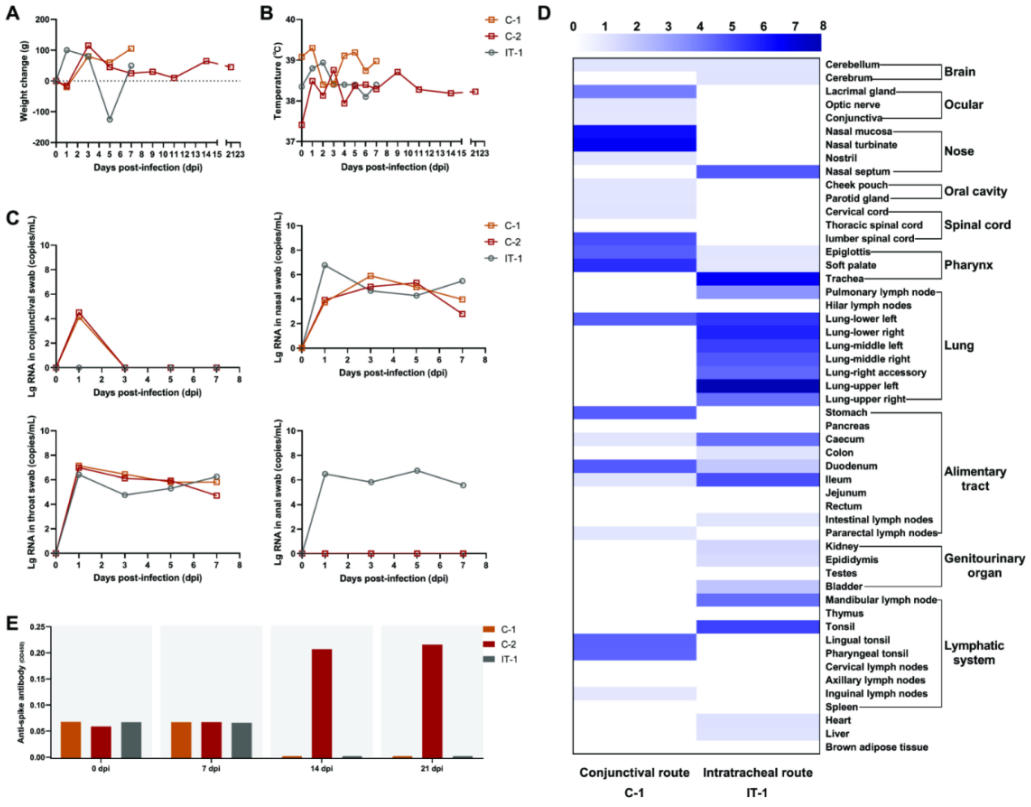

Figure 1. Clinical features, viral distribution and antibody detection in the sera of the SARS-CoV-2-inoculated-rhesus macaques via conjunctival route and intratracheal route, respectively. A and B. Clinical signs including body weight and temperature were observed. C. Viral load of the conjunctival, nasal, throat, and anal swabs specimens from the three inoculated-rhesus macaques 0, 1, 3, 5, and 7 dpi. D. The comparison of viral distributions in the majority organs and tissues from the

209 euthanized and autopsied rhesus macaques inoculated via conjunctival route and
210 intratracheal route on day 7 post-infection. The darker the blue color, the higher the
211 viral load. E. The specific IgG antibody against SARS-CoV-2 in the sera of the
212 inoculated-rhesus macaques was tested on 0, 7, 14, and 21 dpi. All data are presented
213 as mean ± SEM in triplicate experiments. C-1 and C-2 were the two macaques that
214 inoculated with the conjunctival route, IT-1 was the macaque that inoculated with the
215 intratracheal route.

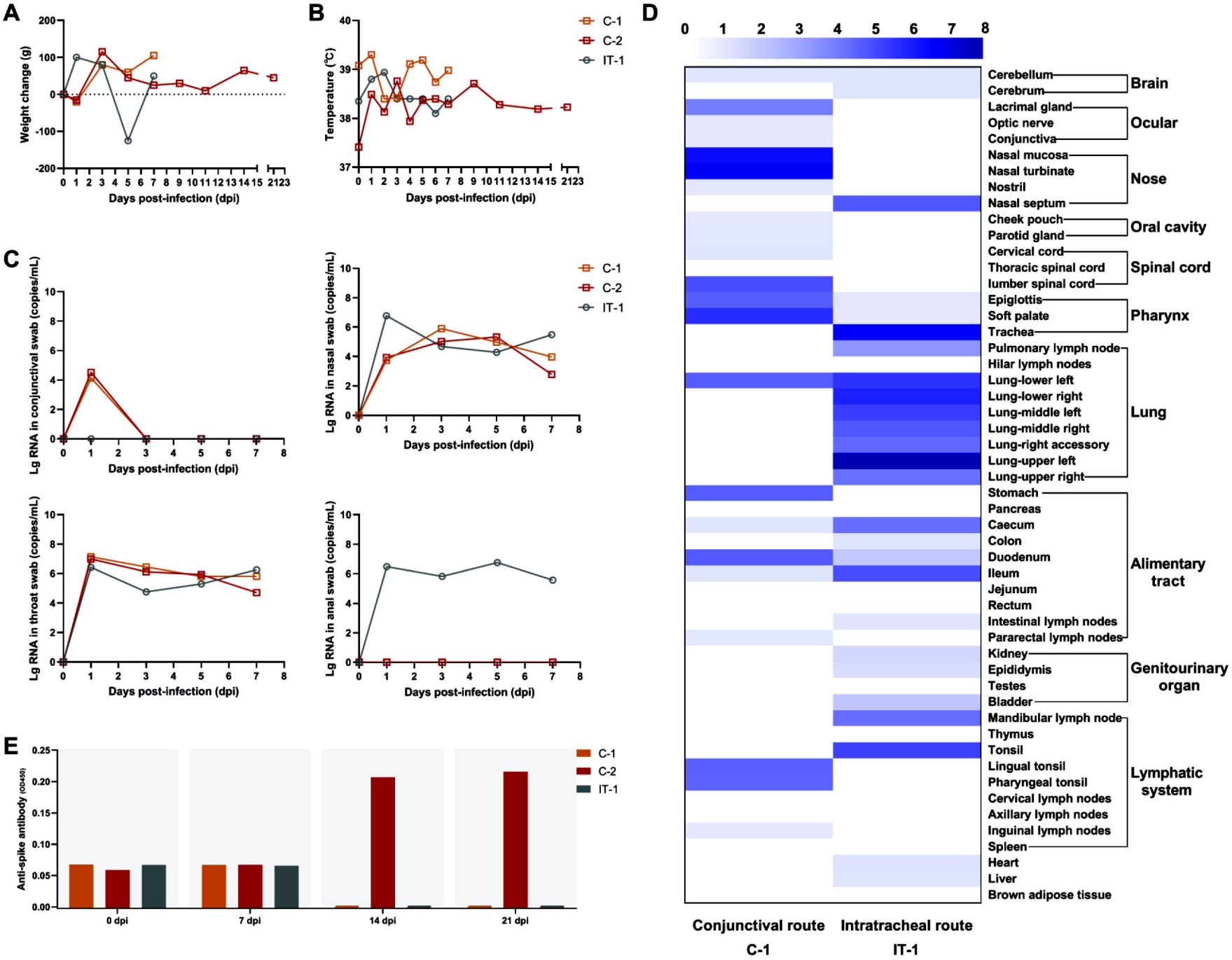
A
Weight change (g)
Days post-infection (dpi)
B
Temperature (℃)
Days post-infection (dpi)
C-1
C-2
IT-1
C
Lg RNA in conjunctival swab (copies/mL)
Days post-infection (dpi)
Lg RNA in nasal swab (copies/mL)
Days post-infection (dpi)
Lg RNA in throat swab (copies/mL)
Days post-infection (dpi)
Lg RNA in anal swab (copies/mL)
Days post-infection (dpi)
D
Cerebellum
Cerebrum
Brain
Lacrimal gland
Optic nerve
Conjunctiva
Ocular
Nasal mucosa
Nasal turbinate
Nostril
Nasal septum
Nose
Cheek pouch
Parotid gland
Oral cavity
Cervical cord
Thoracic spinal cord
lumber spinal cord
Spinal cord
Epiglottis
Soft palate
Trachea
Pharynx
Pulmonary lymph node
Hilar lymph nodes
Lung-lower left
Lung-lower right
Lung-middle left
Lung-middle right
Lung-right accessory
Lung-upper left
Lung-upper right
Lung
Stomach
Pancreas
Caecum
Colon
Duodenum
Ileum
Jejunum
Rectum
Intestinal lymph nodes
Pararectal lymph nodes
Alimentary tract
Kidney
Epididymis
Testes
Bladder
Genitourinary organ
Mandibular lymph node
Thymus
Tonsil
Lingual tonsil
Pharyngeal tonsil
Cervical lymph nodes
Axillary lymph nodes
Inguinal lymph nodes
Spleen
Lymphatic system
Heart
Liver
Brown adipose tissue
Conjunctival route
C-1
Intratracheal route
IT-1
E
Anti-spike antibody (OD450)
0 dpi
7 dpi
14 dpi
21 dpi
C-1
C-2
IT-1